The control of *foxN2/3* expression in sea urchin embryos and its function in the skeletogenic gene regulatory network

Ho Kyung Rho and David R. McClay*

SUMMARY

Early development requires well-organized temporal and spatial regulation of transcription factors that are assembled into gene regulatory networks (GRNs). In the sea urchin, an endomesoderm GRN model explains much of the specification in the endoderm and mesoderm prior to gastrulation, yet some GRN connections remain incomplete. Here, we characterize FoxN2/3 in the primary mesenchyme cell (PMC) GRN state. Expression of *foxN2/3* mRNA begins in micromeres at the hatched blastula stage and then is lost from micromeres at the mesenchyme blastula stage. *foxN2/3* expression then shifts to the non-skeletogenic mesoderm and, later, to the endoderm. Here, we show that Pmar1, Ets1 and Tbr are necessary for activation of *foxN2/3* in micromeres. The later endomesoderm expression of *foxN2/3* is independent of the earlier expression of *foxN2/3* in micromeres and is independent of signals from PMCs. FoxN2/3 is necessary for several steps in the formation of the larval skeleton. Early expression of genes for the skeletal matrix is dependent on FoxN2/3, but only until the mesenchyme blastula stage as *foxN2/3* mRNA disappears from PMCs at that time and we assume that the protein is not abnormally long-lived. Knockdown of FoxN2/3 inhibits normal PMC ingression and *foxN2/3* morphant PMCs do not organize in the blastocoel and fail to join the PMC syncytium. In addition, without FoxN2/3, the PMCs fail to repress the transfating of other mesodermal cells into the skeletogenic lineage. Thus, FoxN2/3 is necessary for normal ingression, for expression of several skeletal matrix genes, for preventing transfating and for fusion of the PMC syncytium.

KEY WORDS: Gene regulatory network, Sea urchin, Forkhead transcription factor, Specification

INTRODUCTION

The sea urchin micromere gene regulatory network (GRN) is one of the best understood of all metazoan embryonic networks (Ettensohn et al., 2007; Oliveri et al., 2002; Oliveri et al., 2003; Oliveri et al., 2008). It specifies the large micromeres toward a skeletogenic fate. Micromeres initiate specification earlier than most cells of the embryo and their GRN operates in a largely cell-autonomous manner. At the early mesenchyme blastula stage, micromeres ingress into the blastocoel by an epithelial-mesenchymal transition (EMT) and differentiate into PMCs. They migrate inside the blastocoel with predictable behavior (Malinda and Ettensohn, 1994; Malinda et al., 1995; Peterson and McClay, 2003) and eventually form a characteristic ring surrounding the archenteron with two ventrolateral clusters gathering to initiate skeletogenesis. The ring of PMCs fuses to form a syncytium before it produces the larval skeleton. The micromere GRN model attempts to explain each step of micromere specification from the birth of micromeres at the fourth cleavage to ingression and begins to explain parts of the terminal differentiation into skeletogenic cells.

Micromere specification is launched when β-catenin enters micromere nuclei starting at the fourth cleavage, and, with maternal Otx, activates *pmar1*, which is a transcriptional repressor and one of the earliest activated PMC-specific transcription factors (Logan et al., 1999; Oliveri et al., 2003). Pmar1 represses a ubiquitous repressor, *hesC*, thereby providing a double-repression gate that

activates micromere-specific genes (Revilla-i-Domingo et al., 2007). Recent data suggest a delay in the repression of *hesC*, indicating that at least some of the downstream transcription factors are activated independently of the Pmar1/*hesC* gate (Sharma and Ettensohn, 2010). As a consequence of these early events, transcription factors including Alx1, Ets1 and Tbr are activated (Croce et al., 2001; Ettensohn et al., 2003; Fuchikami et al., 2002; Kurokawa et al., 1999; Revilla-i-Domingo et al., 2007). Knockdown (KD) of early micromere transcription factors (TFs), such as *alx1*, results in impaired PMC ingression, repressed skeletogenic gene expression and malformed larval skeletons. Perturbation of these early-activated TFs at the top of the GRN thus causes catastrophic failures, whereas TFs activated at later stages of specification produce more specific responses if knocked down. For example, Snail and Twist, which are expressed in micromeres after the hatched blastula stage, play crucial roles during PMC ingression (Wu and McClay, 2007; Wu et al., 2008). Rather than regulating ingression, TFs like Hex or Tgif instead control skeletogenesis and biomineralization through activation of skeletogenic genes such as *msp130*, *sm30* and *sm50* (Oliveri et al., 2008). Thus, understanding the specification and differentiation of PMCs requires one to understand the sequential construction of the PMC network.

Despite an advanced level of understanding of the micromere GRN, there are a number of questions that remain to be answered. For example, the current micromere GRN model includes *foxN2/3*, although the only input modeled is β-catenin, and the only output is *neuralized*, a regulator of *delta* signaling (http://sugp.caltech.edu/endomes/; August 12, 2010). As *foxN2/3* is expressed many hours after β-catenin enters the nuclei of micromeres, we suspected that inputs to *foxN2/3* were incomplete. Also, the FoxN2/3-*neuralized* relationship was based on a

Department of Biology, Duke University, Durham, NC 27708 USA.

*Author for correspondence (dmcclay@duke.edu)

quantitative polymerase chain reaction (QPCR) survey reported a number of years ago, and no detailed studies of *foxN2/3* had been done beyond that survey. For that reason, we decided to investigate how FoxN2/3 works in the micromere GRN in greater detail.

fox genes are members of the Forkhead TF family, which is characterized by a highly conserved forkhead/winged-helix motif, a helix-turn-helix motif consisting of three helices and two large loops (or wings) with DNA binding activity (Clark et al., 1993; Kaestner et al., 2000; Kaufmann et al., 1994; Li and Tucker, 1993). Compared with other *fox* TF subfamilies, the *foxN* subfamily members were discovered more recently. In mammals, the *foxN* subfamily has six members: *foxN1* (Nehls et al., 1994), *foxN2* (human T-cell leukemia virus enhancer factor, HTLF) (Li et al., 1992), *foxN3* (checkpoint suppressor, CHES1) (Pati et al., 1997; Scott and Plon, 2003), *foxN4* (Gouge et al., 2001), *foxN5* (*foxR1*) (Katoh, 2004a) and *foxN6* (*foxR2*) (Katoh, 2004b). *foxN1* is widely known because a *foxN1* mutation produces the immune-deficient nude mice. In sea urchin, 22 *fox* genes were identified from the *Strongylocentrotus purpuratus* genome by searching for the conserved forkhead motif, and two members of the *foxN* subfamily were found: *foxN1/4* and *foxN2/3* (Tu et al., 2006).

In this study, *foxN2/3* was cloned from *Lytechinus variegatus* and its regulation and function were investigated. We found that *foxN2/3* expression in micromeres is regulated by Pmar1, Ets1 and Tbr; *foxN2/3* is also expressed in the non-skeletogenic mesoderm territory and later in the endoderm in an expanding torus pattern. However, that expanding torus of *foxN2/3* expression is not dependent on the Blimp1-Wnt-Otx subcircuit that was recently published for several other endomesoderm genes (Smith et al., 2008; Smith et al., 2007). Micromere progeny require FoxN2/3 to ingress in a timely manner and without FoxN2/3 PMCs fail to join the syncytium, and fail to block transfating. In addition, FoxN2/3 is necessary for activation of the early expression of many PMC specific genes.

MATERIALS AND METHODS

Animals
Lytechinus variegatus adults were obtained from Sea Life (Tavernier, FL, USA) or from Maria Wise (Duke University Marine Laboratory at Beaufort, NC, USA). Gametes were obtained by 0.5M KCl injection. After fertilization, embryos were cultured in artificial sea water at 23°C or room temperature.

Morpholino antisense oligonucleotides (MASO), mRNA injections and drug treatments
Two *LvfoxN2/3*-specific MASOs were obtained from Gene Tools (*foxN2/3* MASO 1: TTCTGGCTTGCGATTAGGAGGCATG; *foxN2/3* MASO 2: AGATTTTTGCCCTTGATTCGCCTTC). *foxN2/3* MASO 1 was injected at 0.5 mM or 0.7 mM and *foxN2/3* MASO 2 was injected at 1 mM. Both caused identical phenotypes and identical gene knockdown consequences. The *alx1* MASO was injected at 1 mM (Ettensohn et al., 2003). The *blimp1b* MASO (CAGAGAAAGTAGAAGAATGTCCGCT or CCCTTTCCTTCGAAAACACAACAGC) was injected at 1 mM and a *tbr* MASO (ATCTCGAAAAAAAGAAATCGCGCCA) was injected at 0.5 mM. Standard control MASO (CCTCTTACCTCAGTTACAATTTATA, Gene Tools) was injected at 0.5-1 mM according to the experimental MASO concentration. Controls for novel morpholinos are presented in the text and supplementary figures. *foxN2/3* CDS was cloned to pCS2 vector and transcribed using the mMessage Machine Kit (Ambion). *pmar1*, *Dn-notch*, and *Dn-Ets1* mRNA were transcribed as described previously (Sharma and Ettensohn, 2010; Sherwood and McClay, 1999; Wu and McClay, 2007). U0126 (Promega) was dissolved in DMSO and added to cultures from early cleavage stages at 10-30 µM.

Micromere-transplantation experiments
Micromere transplantations were performed at the 16-cell or 32-cell stage. Detailed procedures were followed as described previously (Logan et al., 1999).

QPCR
Total RNA was isolated using Trizol (Invitrogen) or the RNeasy Mini Kit (Qiagen). Reverse transcription was performed with a Taqman RT-PCR kit (Applied Biosystems) or iScript cDNA synthesis kit (BioRad). QPCRs were performed using Mastercycler (Eppendorf) with Power SYBR Green PCR Master Mix (Applied Biosystems). The CT (crossing point threshold) was normalized using ubiquitin.

Immunostaining
Embryos were fixed in ice cold methanol for 1 minute, then washed four times in PBST, blocked in 4% normal sheep serum (NSS) in PBST for 30 minutes and incubated in 1d5 mouse antibody (anti MSP-130) (1:200) in 4% NSS PBST overnight at 4°C. After washing four times in 4% NSS PBST, samples were incubated in Cy2-conjugated secondary antibodies (Jackson Laboratories) (1:200) for 30 minutes, and washed in 4% NSS PBST four times and imaged in 50% glycerol and 50% PBST using Zeiss LSM510 confocal microscope.

In situ hybridization
Chromogenic in situ hybridization was performed using standard methods, with DIG-labeled RNA probes and NBT/BCIP (Roche). For double fluorescence in situ hybridization, digoxigenin-11-UTP and fluorescein-12-UTP (Roche) tagged probes were used at 1 ng/1 µl and detected with Cy3-tyramide and fluorescein-tyramide reagents using the TSA-plus Kit (Perkin Elmer). Hybridization and washing were carried out at 65°C. All samples were imaged with a Zeiss Axioplan2 microscope.

RESULTS

Identification and cloning of *L. variegatus foxN2/3*
A fragment of *LvfoxN2/3* was cloned by PCR from a cDNA pool of *L. variegatus*, using primers designed from the *S. purpuratus* sequence. The 5′ UTR was obtained by RACE PCR. The nucleotide sequences of *L. variegatus* and *S. purpuratus* were highly similar (87%) except the first exon, which covers part of the 5′ UTR.

Based on the expected open reading frame from the sequence data, *LvfoxN2/3* encodes a 534 amino acid protein with a forkhead domain located from residue 125 to 212 (http://www.expasy.ch/prosite/; accession number HQ127623). The overall similarity of the amino acid sequences of *L. variegatus foxN2/3* and *S. purpuratus foxN2/3* was 93%, with 100% similarity in the forkhead domain (see Fig. S1A in the supplementary material). Phylogenetic analysis showed that *LvfoxN2/3* clusters with *foxN2* and *foxN3* of Chordates; the amino acid sequence of the forkhead domain was highly conserved (see Fig. S1B in the supplementary material). Other than the forkhead domain, no other apparent domains were found, but the N-terminal and C-terminal regions showed somewhat similar sequences between *LvfoxN2/3* and Chordate *foxN2* or *foxN3* with 30% overall similarity.

Expression pattern of *foxN2/3*
The early expression pattern of *L. variegatus foxN2/3* was similar to that previously reported for *S. purpuratus* (Tu et al., 2006), and with time the expression sites changed dynamically. Whole-mount in situ hybridization (WMISH) showed that *foxN2/3* mRNA appears in micromeres at the hatched blastula stage and disappears from these cells immediately before the mesenchyme blastula stage two hours later (Fig. 1A-F). At the early mesenchyme blastula stage, *foxN2/3* mRNA was observed in the remaining non-skeletal
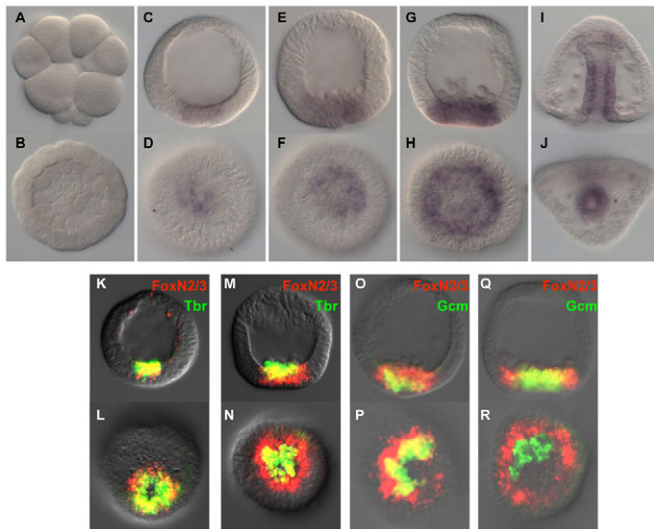
Fig. 1. Dynamic expression pattern of FoxN2/3 in the endomesoderm. (**A-J**) Whole-mount in situ hybridization of *foxN2/3*. At the 16- and 128-cell stages, *foxN2/3* is not expressed (A,B). At the hatched blastula stage, *foxN2/3* is expressed in the vegetal plate (C,D). At the mesenchyme blastula stage, *foxN2/3* is gone from the ingressed PMCs and is expressed in the remaining mesoderm (E,F). By the end of mesenchyme blastula stage, *foxN2/3* is expressed in endodermal cells (G,H). By late gastrula stage, *foxN2/3* is expressed in the mid- and hindgut, with the foregut displaying weak *foxN2/3* expression (I,J). (**K-R**) Double fluorescence in situ hybridization of *foxN2/3* with tissue specific markers. *foxN2/3* expression is compared with the PMC marker *tbr* at the hatched blastula stage (K,L) and early mesenchyme blastula stage (M,N) and with the NSM marker *gcm* at the early mesenchyme blastula stage (O,P) and late mesenchyme blastula stage (Q,R). C, E, G, I, K, M, O and Q show the lateral view and D, F, H, J, L, N, P and R show the vegetal view. In both P and R FoxN2/3 is expressed in a full ring though the embryos shown focus on the GCM half embryo, making it appear, incorrectly, that FoxN2/3 is expressed asymmetrically. The full ring can be seen in F and H.

Fig. 2. *foxN2/3* **expression occurs independently of Blimp1.** (**A-D**) Double fluorescence in situ hybridization of *foxN2/3* (red) and *blimp1* (green) in a hatched blastula (A), mesenchyme blastula (B), early gastrula (C) and late gastrula (D). (**E-H**) Whole-mount in situ hybridization of *foxN2/3*. *blimp1b* MASO-injected embryos (G,H) show no significant difference from control embryos (E,F) in *foxN2/3* expression. HB, hatched blastula; LG, late gastrula.

mesoderm (NSM) cells (Fig. 1E,F), which later form muscle, coelomic pouch, blastocoelar and pigment cells. Over time *foxN2/3* expression was reduced to a low level in the NSM and appeared in endoderm by the late mesenchyme blastula stage (Fig. 1G,H) where it continued to be expressed during archenteron elongation (Fig. 1I,J). A comparison of *foxN2/3* in *L. variegatus* and *S. purpuratus* (Tu et al., 2006) suggests a similar dynamic pattern of expression through development with the exception that in *L. variegatus*, *foxN2/3* mRNA was expressed in the endoderm from the early gastrula stage and remained in the mid- and hindgut area through the late gastrula stage (which was not reported in *S. purpuratus*). Thus, the spatial pattern of *foxN2/3* expression is dynamic and sequentially covers most of the endomesodermal domains over time.

To confirm the lineage assignments, double fluorescence in situ hybridization was performed with *foxN2/3* and two lineage specific markers: *tbr* (a PMC marker) and *gcm* (an NSM marker). At the hatched blastula stage, *foxN2/3* was expressed in the precursors of PMCs as the expression sites of *foxN2/3* and *tbr* were coincident (Fig. 1K,L). At the early mesenchyme blastula stage, as the PMCs ingressed they continued to express *tbr* but eliminated *foxN2/3* (Fig. 1M,N); at the same time, *foxN2/3* expression was present in the mesoderm surrounding PMCs in the vegetal plate where its
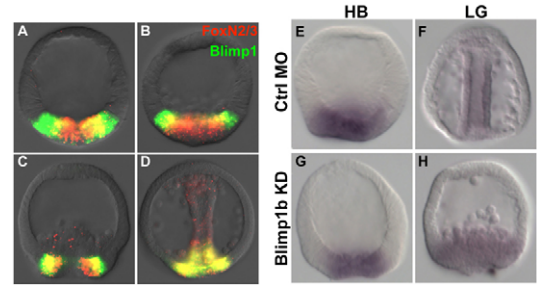
expression overlapped with *gcm* and was observed in some endodermal cells outside *gcm* territory (Fig. 1O,P). At the late mesenchyme blastula stage, transcripts of *foxN2/3* were strongly detected in endodermal cells and greatly reduced in the mesodermal cells in the vegetal plate (Fig. 1Q,R).

Gene regulatory network regulation of *foxN2/3* expression

We next turned to the question of how *foxN2/3* is regulated. The endomesodermal GRN model of August 2010 (http://sugp.caltech.edu/endomes/) indicates only an input from β-catenin to drive *foxN2/3* expression in the micromere lineage. Earlier work showed that β-catenin enters the nuclei of micromeres at the 16-cell stage and is necessary to activate the entire micromere GRN (Logan et al., 1999). This occurs five hours before *foxN2/3* is expressed in the hatched blastula suggesting that TFs downstream of β-catenin later activate *foxN2/3* expression, or are necessary along with β-catenin. The basis for β-catenin as the activator of FoxN2/3 comes from elimination of β-catenin by injection of excess cadherin cytoplasmic tail (Logan et al., 1999; Davidson et al., 2002). With that background in mind, we used the network model to initiate analysis of *foxN2/3* activation and look for additional activators of *foxN2/3*.

Because *foxN2/3* has a dynamic pattern of expression over time, we expected its regulation to be more complex than just an input from β-catenin. Previously, a set of transcription factors including β-catenin, *otx*, *blimp1*, *hox11/13b* and *even-skipped* were shown to have similar expanding torus patterns of expression (Logan et al., 1999; Smith et al., 2008; Smith et al., 2007). Smith et al. showed that a subcircuit composed of *otx*, *wnt8* and *blimp1* work together to produce their characteristic expanding expression pattern (Smith et al., 2007).

As the *foxN2/3* expression region expands behind the expanding *blimp1* expression pattern (Fig. 2A-D), Blimp1 was a promising candidate to regulate the dynamic *foxN2/3* expression pattern. In a test of this hypothesis, however, knockdown of Blimp1b did not inhibit *foxN2/3* expression in the vegetal plate (Fig. 2E-H). As a control for this experiment to verify that the *blimp1b* morpholino blocked Blimp 1 translation, in situ hybridization analysis showed that *blimp1* expression expanded in the presence of the Blimp 1 morpholino, a signature pattern expected of a transcription factor
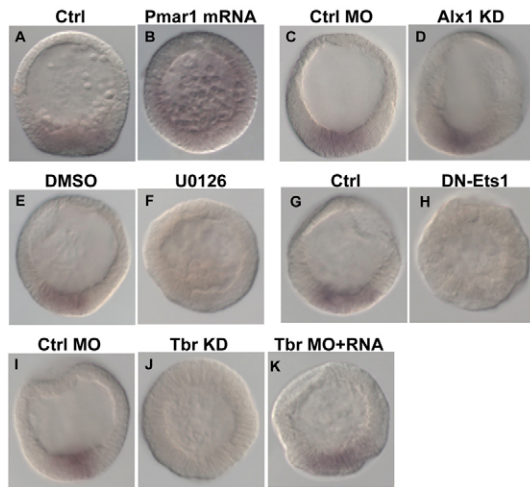
Fig. 3. Regulation of *foxN2/3* expression in micromeres.
(**A-K**) Whole-mount in situ hybridization of *foxN2/3*. Control embryos (A,C,E,G,I) express *foxN2/3* in the vegetal plate at the hatched blastula stage. *Pmar1* mRNA (0.5 μg/μl)-injected embryos (B) express *foxN2/3* in most of the cells. *alx1* MASO-injected embryos (D) show no significant changes in *foxN2/3* expression compared with wild-type embryos (C). U0126 (30 μM)-treated embryos (F), dominant-negative *ets1* mRNA (0.5 μg/μL)-injected (H) and *tbr* MASO-injected embryos (J) show inhibition of *foxN2/3* expression in hatched blastula embryos. Co-injection of *tbr* mRNA (0.5 μg/μL) and MASO (K) shows rescue of *foxN2/3* expression in the vegetal plate.

that represses itself (see Fig. S2A-F in the supplementary material) (Smith et al., 2007; Livi and Davidson, 2006). Further, as expected, the *blimp1b* morpholino also altered the endomesoderm GRN state resulting in a failure of archenteron invagination (see Fig. S2G,H in the supplementary material). Despite the inhibition of Blimp1b, *foxN2/3* continued to be expressed at the vegetal plate of the *blimp1b*-MASO-injected embryos at the same timepoint at which it was expressed in the control embryos, and it later expanded to other endomesodermal cells also. Thus, though *foxN2/3* and the genes in the *blimp1* subcircuit showed highly similar expression dynamics, we conclude that *foxN2/3* expression in micromeres, mesoderm and endoderm does not depend on that subcircuit for its expanding pattern of expression, and therefore it is very unlikely that β-catenin alone is the sole input.

If the *blimp1* expanding torus is not involved, how is *foxN2/3* activated? Here, we focused on activation of FoxN2/3 in the large micromeres. Several candidate PMC-specific transcription factors were chosen based on their position in the micromere GRN. We perturbed each gene and performed WMISH to assess the change of *foxN2/3* expression at the vegetal plate area. First, we tested *pmar1*, one of the earliest transcription factors of PMC specification. According to previous reports (Oliveri et al., 2003; Revilla-i-Domingo et al., 2007), *pmar1* overexpression activates the PMC GRN by repression of the universal repressor *hesC* and transforms almost every cell in the embryo into a PMC. When we overexpressed *pmar1* by mRNA injection, *foxN2/3* expression was indeed induced in most of the cells (Fig. 3B). In other studies, this same result was noted only for micromere GRN genes and not for genes in any of the other cell types (Oliveri et al., 2008). This implies that Pmar1 is a component of the upstream circuit leading to *foxN2/3* expression in PMCs.

However, *pmar1* expression in micromere progeny disappears earlier than the induction of *foxN2/3* and therefore is unlikely to be proximal to *foxN2/3* expression. Thus, we moved on to several candidate transcription factors, each of which is known to be regulated by Pmar1 double repression and expressed earlier than *foxN2/3* induction: *alx1*, *ets1* and *tbr*.

alx1, a PMC-specific transcription factor, is expressed in cells of the large micromere lineage after the fifth cleavage and is maintained by double repression of Pmar1 and/or Ets1. It is involved in early specification of micromeres and regulation of skeletogenic genes (Ettensohn et al., 2003). *alx1* MASO injection inhibited ingression and further skeletogenesis, as expected, but loss of Alx1 did not prevent *foxN2/3* expression in the precursors of PMCs, indicating that Alx1 expression does not occur upstream of *foxN2/3* activation (Fig. 3D).

ets1 is a second downstream target of Pmar1 double repression and is known to be involved in the expression of *alx1* and *tbr*, as well as other skeletogenic genes. Previously, Rottinger et al. showed that Ets1 is activated by phosphorylation, and the inhibition of MAPKK by U0126 prevents Ets1 activity as a transcription factor in the precursors of PMCs (Rottinger et al., 2004). As shown in Fig. 3F, U0126 treatment inhibits *foxN2/3* expression in the precursors of PMCs. As an independent test of an Ets1 input, a dominant-negative construct of Ets1 (Kurokawa et al., 1999; Sharma and Ettensohn, 2010) was tested. Expression of dominant-negative Ets1 blocked *foxN2/3* expression in the micromeres (Fig. 3H). Later, at the mesenchyme blastula stage, *foxN2/3* expression was observed in endomesodermal cells other than micromere/PMCs in embryos expressing dnEts1. This result is consistent with the conclusion that Ets1 is involved only in the expression of *foxN2/3* in micromeres, and not in the other cell types (see Fig. S3B in the supplementary material).

tbr is another transcription factor downstream of Pmar1 and Ets1, and is involved in the early specification of micromeres. Embryos injected with *tbr* morpholinos failed to express *foxN2/3* in micromeres (Fig. 3J). In the same experiment, *tbr* MASO-injected embryos showed normal expression of other markers compared with the controls (see Fig. S4 in the supplementary material). The specificity of the *tbr* MASO was confirmed by a rescue experiment in which the repression of *foxN2/3* by the *tbr* MASO was rescued by co-injection of *tbr* mRNA (Fig. 3K). In the *tbr* MASO-mRNA co-injected embryos and in *tbr* overexpressing (OE) embryos (data not shown), *foxN2/3* expression was limited to the vegetal plate and did not show ectopic expression. This implies that Tbr is not sufficient to induce expression of *foxN2/3* on its own, and requires other PMC-specific transcription factor(s) in an AND logic function (Tbr AND another TF). Thus, in micromeres, Pmar1 probably regulates *foxN2/3* expression through Ets1 and/or Tbr, but not Alx1. As Ets1 also regulates Tbr, we cannot at present distinguish whether Ets1 activates *foxN2/3* directly, or works indirectly through its role in activation of *tbr*. Further, as β-catenin activates *pmar1*, which activates *ets1* and *tbr* through its double repression gate, one cannot conclude that β-catenin has a direct input into activation of *foxN2/3*.

The expression of *foxN2/3* in PMCs, non-skeletogenic mesoderm and endodermal cells can be regulated by either one common induction/repression mechanism similar to the Wnt-Blimp-Otx torus subcircuit, or by different independent mechanisms. We first asked whether *foxN2/3* has an upstream role in the dynamic expression of *foxN2/3* in other cells. Two MASOs were designed and injected into fertilized eggs to inhibit the endogenous translation of *foxN2/3* and both of the MASOs showed similar effects on early development, though the *foxN2/3*
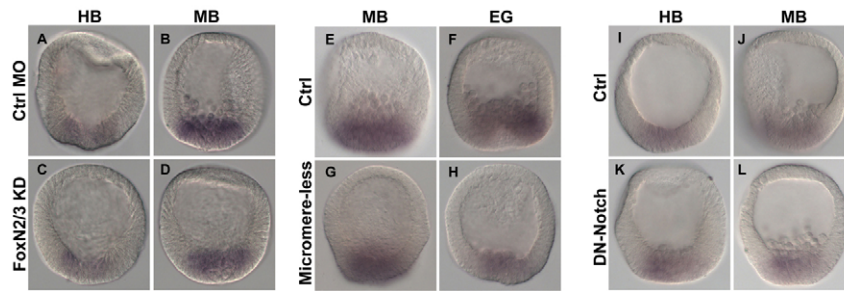
Fig. 4. Regulation of *foxN2/3* expression. (A-L) Whole-mount in situ hybridization of *foxN2/3*. *foxN2/3* MASO-injected embryos (C,D) show no significant difference from control embryos (A,B). Micromereless embryos (G,H) express *foxN2/3* in the vegetal plate area when control embryos express *foxN2/3* in the non-skeletogenic mesoderm (E) or endoderm (F). Control embryos (I,J) and dominant negative *notch* mRNA (0.2 µg/µL)-injected embryos (K,L) express *foxN2/3* at similar levels. EG, early gastrula; HB, hatched blastula; MB, mesenchyme blastula.

MASO 1 optimal dosage was lower than that for *foxN2/3* MASO 2. As controls, the efficiency and specificity of *foxN2/3* MASOs was shown by repression of red fluorescent protein (RFP) using the morpholino complementary to the FoxN2/3 5′ UTR sequence. The expression of FoxN2/3 5′ UTR-connected membrane RFP was eliminated in the presence of the *foxN2/3* morpholino whereas membrane RFP downstream of reverse strand FoxN2/3 5′ UTR was not repressed (see Fig. S5 in the supplementary material). In Fig. 5, another control shows that introduction of FoxN2/3 mRNA rescues the FoxN2/3 MASO. Thus, the morpholinos, by those tests, are efficient and specific for blockage of FoxN2/3 translation.

When *foxN2/3* translation was blocked by MASO injection, *foxN2/3* was still transcribed at the vegetal pole area at the hatched blastula stage (Fig. 4A-D). Importantly, its expression expanded to adjacent cells later and QPCR results also showed that the expression level of *foxN2/3* was not significantly changed by *foxN2/3* MASOs (ΔΔCt<2). These results indicate that FoxN2/3 does not regulate itself, nor does its expression in one set of cells participate in the expanding torus pattern of *foxN2/3* expression, i.e. later expression does not depend on the earlier expression. As an independent test of this hypothesis, when we removed micromeres at the 16-cell stage, *foxN2/3* was still expressed in the vegetal plate at roughly the same time that *foxN2/3* was expressed in the non-skeletogenic mesoderm of control embryos (Fig. 4E-H). Thus, *foxN2/3* expression in non-skeletogenic mesoderm cells is not dependent on FoxN2/3 expression in micromeres. Moreover, its expression is not dependent on signals from the micromeres. Because Delta is known to be important for NSM specification, perturbation of Delta signaling from micromeres was tested and the results suggest that FoxN2/3 is activated in NSM independent of Delta signaling. When the Delta signaling pathway was disrupted by dominant-negative *notch* mRNA or *delta* MASO injection, the embryos showed the albino phenotype as expected from previous reports using these reagents (Croce and McClay, 2010; Sherwood and McClay, 1999; Sweet et al., 2002). However, *foxN2/3* was still expressed in the vegetal plate (Fig. 4I-L; data not shown). Thus, the later expression of foxN2/3 requires an independent mechanism that is not dependent on earlier *foxN2/3* expression in micromeres, nor from the micromere-released signals, including activation of Delta in the NSM. *foxN2/3* has at least one PMC-specific cis-regulatory module that is regulated by Ets1 and/or Tbr, and as Tbr is only expressed by micromeres, this module is not required for the later endomesodermal *foxN2/3*

expression. These results suggest that multiple cis-regulatory modules sequentially regulate activation of *foxN2/3* to produce its dynamic pattern of expression in embryos.

Functional characterization of FoxN2/3 in micromeres

Next, we examined the functional role of FoxN2/3 in micromeres. *foxN2/3* expression was perturbed in a number of experiments with the morpholinos. PMC ingression was not observed in the *foxN2/3* MASO-injected embryos by the time the control embryos had finished PMC ingression (*n*=57/65; Fig. 5A,C). Archenteron invagination in *foxN2/3* MASO-injected embryos was also delayed relative to controls and there was a reduced frequency of fusion to form a stomodeum. Without FoxN2/3, formation of larval skeleton was also disrupted; at 24 hours post fertilization, the control embryos had formed typical elongated spicules, whereas FoxN2/3 KD embryos did not yet have any skeletons (*n*=37/39; Fig. 5B,D). Eventually, spicules were observed in some *foxN2/3* MASO-injected embryos, but the skeleton was disorganized and the length
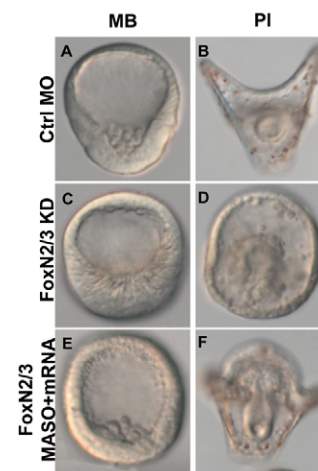

Fig. 5. Perturbation of *foxN2/3* and PMCs. (A,B) Control embryos undergo normal PMC ingression and form the skeleton. **(C,D)** *foxN2/3* MASO-injected embryos show neither ingressed PMCs nor skeleton at the same stage. **(E,F)** Co-injection of *foxN2/3* MASO and FoxN2/3 mRNA rescues ingression and on-time production of skeleton. MB, mesenchyme blastula; Pl, pluteus.
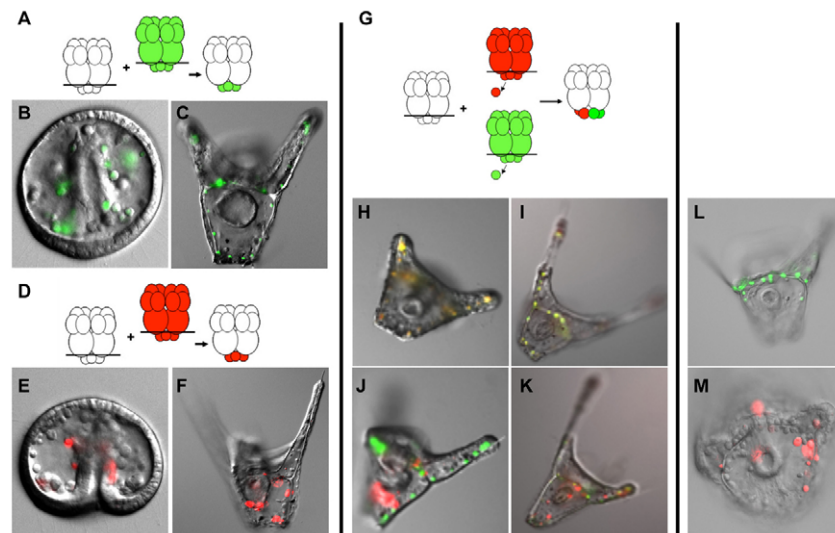
Fig. 6. *foxN2/3* and development of the larval skeleton. (**A-C**) FITC-labeled control micromeres (green) are transplanted into a micromereless embryo (A). The transplanted control micromeres ingress (B) and form a normal skeleton (C). (**D-F**) *foxN2/3* MASO-injected micromeres labeled with rhodamine-conjugated dextran (red) are transplanted into a micromereless control embryo (D). The transplanted *foxN2/3* MASO-injected micromeres reach the blastocoel eventually, but remain unorganized in the blastocoel and fail to form skeletons, though a skeleton forms from unstained cells (E,F). (**G-K**) Mixed micromere transplantation experiments are described schematically in G. Two transplanted red control and two green control micromeres form a syncytium resulting in yellow cells along the skeleton (H,I). Red *foxN2/3* MASO-injected micromeres remain unorganized in the blastocoel whereas green control micromeres form the larval skeleton (J,K). (**L,M**) Micromere transplantation experiments with the *tbr* MASO. Transplanted control micromeres form normal skeletons (L). Transplanted *tbr* MASO injected micromeres fail to form skeletons (M).

of the spicules was shorter than that of the controls. As the MASO concentration was increased, the spicule defects became more severe. Thus, reduction of FoxN2/3 caused a delay or loss of skeletogenesis and endoderm development. In addition, overexpression of FoxN2/3 by mRNA injection caused precocious ingression with little delay of archenteron development but showed no further defects (data not shown). Given this preliminary survey of visible phenotypes upon perturbations, we next turned to experimental analysis of function in a more targeted approach at a cellular and molecular level.

FoxN2/3 is necessary for syncytium formation and for inhibition of transfating

To focus on the PMC-specific function of FoxN2/3, experiments were designed so that *foxN2/3* MASOs were exclusively carried by PMCs. For this cell-specific inquiry, micromere transplantation experiments combined micromeres from MASO-injected embryos with control micromereless (micromere-removed) embryos (Fig. 6A-F). As controls, four unperturbed micromeres labeled with the fluorescent dye FITC were transplanted to unlabeled micromereless embryos. The descendants of those control micromeres underwent normal skeletogenesis and cells with green fluorescence were located along the larval skeleton (Fig. 6A-C). By contrast, PMCs originating from *foxN2/3* MASO-injected micromeres remained in the blastocoel without contributing to the larval skeleton (Fig. 6D-F). Surprisingly, whereas the FoxN2/3 KD micromeres failed to form skeleton, the recombinant embryos had a normal skeleton produced by cells without fluorescent dye (*n*=3/3 and 3/4, two independent experiments; Fig. 6F). These data suggested that the skeletogenic cells had not originated from the transplanted micromeres, but instead had transfated from endomesodermal cells of the host embryo. In the absence of PMCs, other mesoderm cells are known to transfate to PMCs and form the skeleton (Ettensohn and McClay, 1988). Thus, the

presence of these transfated cells suggests that in the absence of FoxN2/3 in micromeres, there is a failure to send signals that usually inhibit the transfating of non-skeletogenic mesoderm cells. Further, these results imply that FoxN2/3 is required for syncytium formation, as FoxN2/3 KD PMCs failed to participate in the transfated syncytium.

To challenge experimentally the question of syncytium formation even more directly, a mixed micromere experiment was performed. First, two red control and two green control micromeres were transplanted at the 16-cell stage into the space left behind by removal of micromeres from an unlabeled host (Fig. 6G). After the formation of syncytium, the red and green fluorescent dyes mixed in the syncytium and resulted in yellow cells along the larval skeleton (Fig. 6H,I), indicating that the control red and control green cells had collaborated in syncytium formation. By contrast, when two red micromeres injected with *foxN2/3* MASO were transplanted along with two control green micromeres, the green PMCs contributed to the skeleton, but the FoxN2/3 KD PMCs remained in the blastocoel separate from the skeleton (*n*=3/3 and 1/2, two independent experiments; Fig. 6J,K). Thus, knockdown of FoxN2/3 in PMCs resulted in a failure of these cells to be incorporated into the syncytium, explaining at least one of the reasons that the larval skeleton is malformed in FoxN2/3 KD embryos.

As a further independent test, as the function of FoxN2/3 was shown to be downstream of Tbr, we predicted that knockdown of Tbr should also produce some, if not all, of the defects shown by knockdown of FoxN2/3. Accordingly, the same micromere transplant experiments were performed with the *tbr* morphants (Fig. 6L,M). As would be predicted if *tbr* is a major regulator of *foxN2/3*, *tbr* morphant PMCs also failed to produce a larval skeleton and failed to prevent non-skeletogenic mesoderm transfating; the recombinant embryos had a normal skeleton produced by cells without fluorescent dye (*n*=3/3 and 3/3, two independent experiments; Fig. 6M).
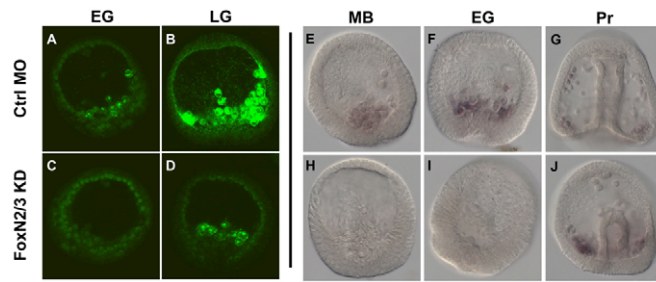
Fig. 7. *foxN2/3* and PMC-specific gene expression. (**A-D**) 1d5 immunostaining labeling Msp130. Msp130 is expressed in the control embryo in the PMCs at the early gastrula stage (A,B). Msp130 expression is greatly delayed in *foxN2/3* MASO-injected embryos (C,D). (**E-J**) Whole-mount in situ hybridization of *VEGFR*. *VEGFR* is expressed in the ingressed PMCs of control embryos (E-G). *VEGFR* is not expressed in *foxN2/3* KD embryos (H,I), but appears later (J). EG, early gastrula; LG, late gastrula; MB, mesenchyme blastula; Pr, prism.

FoxN2/3 is necessary for skeletogenic gene expression

To understand further the molecular function of FoxN2/3 in PMCs, we looked at the expression of potential downstream target genes of FoxN2/3 in the PMC GRN. First, Msp130, a PMC-specific cell-surface glycoprotein involved in skeletogenesis, was examined by immunostaining (Fig. 7A-D). *foxN2/3*-MASO injected embryos showed no expression of Msp130 ~12 hours after fertilization, when control embryos showed a high level of Msp130 in PMCs (Fig. 7A,C). Eventually, Msp130 expression was recovered in ingressed cells of foxN2/3 KD embryos (Fig. 7D, 20 hours after fertilization); whether these MSP130-expressing cells were the original PMCs or transfated PMCs was not determined, but the expression coincided with the appearance of the transfated PMCs in micromere-removed embryos (Ettensohn and McClay, 1988). When we examined other skeletogenic genes by QPCR in FoxN2/3 KD embryos, *sm30* and *sm50* expression levels were also strongly reduced, consistent with the hypothesis that many skeletogenic genes require FoxN2/3 input (Table 1). Eventually, expression of the skeletogenic genes assayed, i.e. MSP130, *sm30* and *sm50*, recovered in later stages of FoxN2/3 KD embryos. Again, that 'recovery' might instead have been expression by transfated PMCs. In either case, these results indicate that FoxN2/3 is necessary for the early expression of skeletogenic genes. Another FoxN2/3 target was the VEGF Receptor (VEGFR), which is known to be involved in the proper organization of larval skeleton (Duloquin et al., 2007). WMISH showed that the expression of *VEGFR* in the PMCs is absent in FoxN2/3 KD embryos whereas the control embryos showed *VEGFR* signal in the ingressed PMCs (Fig. 7E-I). In FoxN2/3 KD embryos, *VEGFR* expression recovered during later gastrulation, just as other skeletogenic genes recover (Fig. 7J).

Table 1. Effect of *foxN2/3* morpholino antisense oligonucleotides (MASO) MO1 and MO2 on expression of the skeletogenic genes *sm30* and *sm50*

	FoxN2/3 MO1 (ΔΔCt)	FoxN2/3 MO2 (ΔΔCt)
sm30	–6.20/–7.02	–2.66/–3.45
sm50	–4.42/–8.52	–1.91/–2.51

Embryos were harvested at the mesenchyme blastula stage. CT (crossing point threshold) values determined by quantitative polymerase chain reaction were normalized by ubiquitin and ΔΔCt values were calculated by subtracting the sample from the control. Two separate sets of experiments are shown.

foxN2/3 mRNA normally disappears from PMCs after ingression though its protein might persist for a short time. Thus, although FoxN2/3 is part of the GRN that activates skeletogenic genes and the *VEGFR*, it is not likely to be involved in long-term maintenance of that expression. In the endomesoderm GRN model of *S. purpuratus*, expression of the skeletogenic genes is driven by a massively parallel set of inputs; our results suggest that FoxN2/3 is one of those inputs and a number of those inputs continue to be expressed after ingression. Nevertheless, even though micromere FoxN2/3 is lost shortly after ingression, the new status of the GRN depends on the earlier GRN state that included FoxN2/3 as an important TF input.

DISCUSSION
Control of *foxN2/3* expression in micromeres

The dynamic expression pattern of FoxN2/3 is similar to the subcircuit of Blimp1, Wnt8 and Otx, as well as to their downstream genes including *hox11/13b* and *eve* (Smith et al., 2008; Smith et al., 2007). However, knockdown of Blimp1b failed to inhibit the *foxN2/3* expression pattern. Instead, in micromeres, *foxN2/3* expression requires Ets1 and Tbr, downstream of Pmar1 and β-catenin, for its activation. We cannot rule out a direct input from either the Pmar1 double repression system or β-catenin, though by the time FoxN2/3 is activated expression of both factors is reduced or absent in micromeres. Both, however, are upstream of expression of Ets1 and Tbr, the two TFs shown to be required and expressed at the time of FoxN2/3 activation. Inhibition of Ets1 activation or knockdown of Tbr did not inhibit *foxN2/3* expression in non-skeletogenic mesoderm or endoderm cells, indicating that control of expression of *foxN2/3* in skeletogenic mesoderm is independent of regulatory mechanisms controlling *foxN2/3* elsewhere in the embryo. We were surprised to learn that in the mesoderm, *foxN2/3* is activated independent of the Delta signal that is necessary for several core transcription factors of the NSM network subcircuit (Sherwood and McClay, 1999; Sweet et al., 2002). The endodermal expression of *foxN2/3* beginning at mesenchyme blastula diverges into weak expression in the foregut and stronger expression in the mid/hindgut area during late gastrulation; this pattern implies that yet other regulatory modules exist in the *foxN2/3* enhancer distinct from the mesodermal control module. Thus, our data suggest that at least three different cis-regulatory modules are employed for the expression of *foxN2/3* during early development up to gastrulation.

This study on *foxN2/3* expression highlights the benefits of using a GRN model as a guide to elucidate regulatory interactions. The PMC GRN provided a logical framework, allowing us to focus our efforts on candidates for the regulators of *foxN2/3* expression in PMCs. Pmar1 is one of the earliest PMC-specific transcription factors activated by β-catenin nuclear localization and it regulates most downstream PMC-specific genes. Thus, it was expected that Pmar1 would be necessary for *foxN2/3* expression in PMCs also, and our results support that hypothesis. The PMC GRN also provided candidates to explain the temporal difference between the modeled Pmar1 input, and the actual time of *foxN2/3* activation. We predicted that *foxN2/3* expression requires additional inputs from other components of the micromere GRN. The prior information quickly led us to Ets1 and Tbr, which were found to regulate *foxN2/3* expression in PMCs. Thus, the PMC GRN was utilized as a map to find the proper niche of the gene in the PMC specification cascade. By extension, any gene can be examined in this way to find its position in the network, using the prior knowledge contained in GRN models.

Function of FoxN2/3 in micromeres and PMCs

Immunostaining, QPCR and WMISH data show that FoxN2/3 KD prevents the early expression of skeletogenic genes and other PMC-specific genes as part of what has been described as a parallel input of a number of transcription factors (Peter and Davidson, 2009). Thus, FoxN2/3 is indispensable for the circuitry controlling PMC differentiation genes. This circuitry takes the appearance of many parallel inputs because the GRN is responsible for activation of all PMC differentiation genes. Some of the PMC differentiation genes are known to receive direct inputs from a subset of those transcription factors, but unless a detailed cis-regulatory analysis is done it is not possible to distinguish between a requirement for the TF as part of a competent GRN state and a direct requirement for the TF in activation of specific downstream genes. Expression of *foxN2/3* is extinguished in PMCs shortly after ingression. These data suggest that the importance of FoxN2/3 in the micromeres is in achieving a competent GRN state rather than directly contributing to activation of the downstream genes. Of course this does not rule out possible direct inputs from FoxN2/3 into the differentiation genes, but if FoxN2/3 provides direct input, it must transfer continuing expression of those genes to other transcription factors shortly thereafter because it disappears from PMCs.

As shown previously, knockdown of the VEGF receptor (VEGFR) results in failure to produce a skeleton in embryos (Duloquin et al., 2007). Here, the data show that knockdown of FoxN2/3 in micromeres causes a large reduction in *VEGFR* expression by PMCs, yet eventually the embryos produce a skeleton. This was puzzling until we learned that transfated mesoderm cells produced the skeletons in FoxN2/3 KD embryos. However, in those experiments the transfated PMCs made a skeleton although the FoxN2/3 MASO was present in those cells also, implying that as a result of transfating, the neo-PMCs somehow got around the FoxN2/3-knockdown block to synthesize the VEGFR. This result implies both that FoxN2/3 is an indirect input into expression of the VEGFR, and that the transfating mechanism employs a network that no longer requires FoxN2/3. Indeed, it was shown earlier that transfated PMCs also do not require Pmar1 (Ettensohn et al., 2007). As we show that *foxN2/3* expression is downregulated at ingression, yet in normal PMCs the suite of differentiation genes continues to be expressed, including *VEGFR*, apparently transfated PMCs are able to drive expression of those differentiation genes by somehow bypassing FoxN2/3.

In this study, FoxN2/3 is shown to be involved in PMC organization, fusion, differentiation and cell-to-cell signaling. FoxN2/3 is one of a number of transcription factors contributing to the network state that must be reached before differentiation ensues. The diverse consequences seen when FoxN2/3 is perturbed shows the consequence of disturbing the combined regulatory state of a gene regulatory network that collectively controls progression to differentiation of this lineage. If a similar study were performed on other transcription factors modeled to control differentiation (e.g. Tel, Hex or Tgif), the outcome would probably be similar to the findings with FoxN2/3. Single transcription factors might be necessary for, but are very unlikely to singularly regulate, all of these processes; rather it is the system of transcription factors tied together by the GRN that controls those functions. In some cases, these regulatory interactions provide direct inputs into differentiation functions, whereas in other cases, the regulatory interactions are inputs into a later state of the GRN. The current GRN model depicts the inputs into differentiation genes as parallel, and some of these do activate skeletal matrix genes directly (Amore and Davidson, 2006). However, the successive GRN states that first cause differentiation, and then maintain it, remain to be solved in detail.

Competing interests statement
The authors declare no competing financial interests.

Supplementary material
Supplementary material for this article is available at
http://dev.biologists.org/lookup/suppl/doi:10.1242/dev.058396/-/DC1

References
Amore, G. and Davidson, E. H. (2006). cis-Regulatory control of cyclophilin, a member of the ETS-DRI skeletogenic gene battery in the sea urchin embryo. *Dev. Biol.* **293**, 555-564.
Clark, K. L., Halay, E. D., Lai, E. and Burley, S. K. (1993). Co-crystal structure of the HNF-3/fork head DNA-recognition motif resembles histone H5. *Nature* **364**, 412-420.
Croce, J., Lhomond, G., Lozano, J. C. and Gache, C. (2001). ske-T, a T-box gene expressed in the skeletogenic mesenchyme lineage of the sea urchin embryo. *Mech. Dev.* **107**, 159-162.
Croce, J. C. and McClay, D. R. (2010). Dynamics of Delta/Notch signaling on endomesoderm segregation in the sea urchin embryo. *Development* **137**, 83-91.
Davidson, E. H., Rast, J. P., Oliveri, P., Ransick, A., Calestani, C., Yuh, C. H., Minokawa, T., Amore, G., Hinman, V., Arenas-Mena, C. et al. (2002). A genomic regulatory network for development. *Science* **295**, 1669-1678.
Duloquin, L., Lhomond, G. and Gache, C. (2007). Localized VEGF signaling from ectoderm to mesenchyme cells controls morphogenesis of the sea urchin embryo skeleton. *Development* **134**, 2293-2302.
Ettensohn, C. A. and McClay, D. R. (1988). Cell lineage conversion in the sea urchin embryo. *Dev. Biol.* **125**, 396-409.
Ettensohn, C. A., Illies, M. R., Oliveri, P. and De Jong, D. L. (2003). Alx1, a member of the Cart1/Alx3/Alx4 subfamily of Paired-class homeodomain proteins, is an essential component of the gene network controlling skeletogenic fate specification in the sea urchin embryo. *Development* **130**, 2917-2928.
Ettensohn, C. A., Kitazawa, C., Cheers, M. S., Leonard, J. D. and Sharma, T. (2007). Gene regulatory networks and developmental plasticity in the early sea urchin embryo: alternative deployment of the skeletogenic gene regulatory network. *Development* **134**, 3077-3087.
Fuchikami, T., Mitsunaga-Nakatsubo, K., Amemiya, S., Hosomi, T., Watanabe, T., Kurokawa, D., Kataoka, M., Harada, Y., Satoh, N., Kusunoki, S. et al. (2002). T-brain homologue (HpTb) is involved in the archenteron induction signals of micromere descendant cells in the sea urchin embryo. *Development* **129**, 5205-5216.
Gouge, A., Holt, J., Hardy, A. P., Sowden, J. C. and Smith, H. K. (2001). Foxn4-a new member of the forkhead gene family is expressed in the retina. *Mech. Dev.* **107**, 203-206.
Kaestner, K. H., Knochel, W. and Martinez, D. E. (2000). Unified nomenclature for the winged helix/forkhead transcription factors. *Genes Dev.* **14**, 142-146.
Katoh, M. (2004a). Identification and characterization of human FOXN5 and rat Foxn5 genes in silico. *Int. J. Oncol.* **24**, 1339-1344.
Katoh, M. (2004b). Identification and characterization of human FOXN6, mouse Foxn6, and rat Foxn6 genes in silico. *Int. J. Oncol.* **25**, 219-223.
Kaufmann, E., Hoch, M. and Jackle, H. (1994). The interaction of DNA with the DNA-binding domain encoded by the Drosophila gene fork head. *Eur. J. Biochem.* **223**, 329-337.
Kurokawa, D., Kitajima, T., Mitsunaga-Nakatsubo, K., Amemiya, S., Shimada, H. and Akasaka, K. (1999). HpEts, an ets-related transcription factor implicated in primary mesenchyme cell differentiation in the sea urchin embryo. *Mech. Dev.* **80**, 41-52.
Li, C. and Tucker, P. W. (1993). DNA-binding properties and secondary structural model of the hepatocyte nuclear factor 3/fork head domain. *Proc. Natl. Acad. Sci. USA* **90**, 11583-11587.
Li, C., Lusis, A. J., Sparkes, R., Tran, S. M. and Gaynor, R. (1992). Characterization and chromosomal mapping of the gene encoding the cellular DNA binding protein HTLF. *Genomics* **13**, 658-664.
Livi, C. B. and Davidson, E. H. (2006). Expression and function of blimp1/krox, an alternatively transcribed regulatory gene of the sea urchin endomesoderm network. *Dev. Biol.* **293**, 513-525.

Logan, C. Y., Miller, J. R., Ferkowicz, M. J. and McClay, D. R. (1999). Nuclear beta-catenin is required to specify vegetal cell fates in the sea urchin embryo. *Development* **126**, 345-357.

Malinda, K. M. and Ettensohn, C. A. (1994). Primary mesenchyme cell migration in the sea urchin embryo: distribution of directional cues. *Dev. Biol.* **164**, 562-578.

Malinda, K. M., Fisher, G. W. and Ettensohn, C. A. (1995). Four-dimensional microscopic analysis of the filopodial behavior of primary mesenchyme cells during gastrulation in the sea urchin embryo. *Dev. Biol.* **172**, 552-566.

Nehls, M., Pfeifer, D., Schorpp, M., Hedrich, H. and Boehm, T. (1994). New member of the winged-helix protein family disrupted in mouse and rat nude mutations. *Nature* **372**, 103-107.

Oliveri, P., Carrick, D. M. and Davidson, E. H. (2002). A regulatory gene network that directs micromere specification in the sea urchin embryo. *Dev. Biol.* **246**, 209-228.

Oliveri, P., Davidson, E. H. and McClay, D. R. (2003). Activation of pmar1 controls specification of micromeres in the sea urchin embryo. *Dev. Biol.* **258**, 32-43.

Oliveri, P., Tu, Q. and Davidson, E. H. (2008). Global regulatory logic for specification of an embryonic cell lineage. *Proc. Natl. Acad. Sci. USA* **105**, 5955-5962.

Pati, D., Keller, C., Groudine, M. and Plon, S. E. (1997). Reconstitution of a MEC1-independent checkpoint in yeast by expression of a novel human fork head cDNA. *Mol. Cell. Biol.* **17**, 3037-3046.

Peter, I. S. and Davidson, E. H. (2009). Modularity and design principles in the sea urchin embryo gene regulatory network. *FEBS Lett.* **583**, 3948-3958.

Peterson, R. E. and McClay, D. R. (2003). Primary mesenchyme cell patterning during the early stages following ingression. *Dev. Biol.* **254**, 68-78.

Revilla-i-Domingo, R., Oliveri, P. and Davidson, E. H. (2007). A missing link in the sea urchin embryo gene regulatory network: hesC and the double-negative specification of micromeres. *Proc. Natl. Acad. Sci. USA* **104**, 12383-12388.

Rottinger, E., Besnardeau, L. and Lepage, T. (2004). A Raf/MEK/ERK signaling pathway is required for development of the sea urchin embryo micromere lineage through phosphorylation of the transcription factor Ets. *Development* **131**, 1075-1087.

Scott, K. L. and Plon, S. E. (2003). Loss of Sin3/Rpd3 histone deacetylase restores the DNA damage response in checkpoint-deficient strains of Saccharomyces cerevisiae. *Mol. Cell. Biol.* **23**, 4522-4531.

Sharma, T. and Ettensohn, C. A. (2010). Activation of the skeletogenic gene regulatory network in the early sea urchin embryo. *Development* **137**, 1149-1157.

Sherwood, D. R. and McClay, D. R. (1999). LvNotch signaling mediates secondary mesenchyme specification in the sea urchin embryo. *Development* **126**, 1703-1713.

Smith, J., Theodoris, C. and Davidson, E. H. (2007). A gene regulatory network subcircuit drives a dynamic pattern of gene expression. *Science* **318**, 794-797.

Smith, J., Kraemer, E., Liu, H., Theodoris, C. and Davidson, E. (2008). A spatially dynamic cohort of regulatory genes in the endomesodermal gene network of the sea urchin embryo. *Dev. Biol.* **313**, 863-875.

Sweet, H. C., Gehring, M. and Ettensohn, C. A. (2002). LvDelta is a mesoderm-inducing signal in the sea urchin embryo and can endow blastomeres with organizer-like properties. *Development* **129**, 1945-1955.

Tu, Q., Brown, C. T., Davidson, E. H. and Oliveri, P. (2006). Sea urchin Forkhead gene family: phylogeny and embryonic expression. *Dev. Biol.* **300**, 49-62.

Wu, S. Y. and McClay, D. R. (2007). The Snail repressor is required for PMC ingression in the sea urchin embryo. *Development* **134**, 1061-1070.

Wu, S. Y., Yang, Y. P. and McClay, D. R. (2008). Twist is an essential regulator of the skeletogenic gene regulatory network in the sea urchin embryo. *Dev. Biol.* **319**, 406-415.